



MST4 promotes proliferation, invasion, and metastasis of gastric cancer by enhancing autophagy

Pengwei Liu^{a,b}, Lin Li^b, Wei Wang^b, Chiyi He^b, Chunfang Xu^{a,*}

^a Departments of Gastroenterology, The First Affiliated Hospital of Soochow University, Suzhou, 215006, Jiangsu, China

^b Departments of Gastroenterology, The First Affiliated Hospital of Wannan Medical College, Wuhu, 241001, Anhui, China

ARTICLE INFO

Keywords:

Gastric cancer
MST4
Autophagy
Migration and invasion

ABSTRACT

Background: Mammalian infertile-20-like kinase 4 (MST4) plays major roles in the progression of malignant tumor types, but its function in gastric cancer (GC) remains poorly understood.

Objective: To investigate the regulatory mechanism of MST4 in GC.

Methods: Immunohistochemistry was used to detect MST4 protein in GC tissue. Additionally, the correlation between MST4 expression and the clinicopathological characteristics and prognosis of GC was evaluated. The MST4 expression level in GC cells was measured by western blotting and quantitative real-time polymerase chain reaction. Moreover, the regulatory mechanism of MST4 was investigated in vitro and in vivo.

Results: Overexpression of MST4 was found in GC tissue and cell lines, which correlated to the tumor size, histological type, invasion depth, ulcer, lymph node metastasis, lymphovascular invasion, perineural invasion and TNM stage (all $P < 0.01$). In terms of MST4 functions in vitro, its upregulation facilitated the proliferation, migration, and invasion of GC cells. Furthermore, MST4 promoted these processes by facilitating autophagy, whereas downregulation of MST4 significantly attenuated these processes. Downregulation of MST4 also attenuated tumor growth in vivo.

Conclusion: High expression of MST4 indicates a poor prognosis and promotes GC cell proliferation, invasion, and metastasis by enhancing autophagy.

1. Introduction

Gastric cancer (GC), one of the most prevalent malignant digestive tumors, ranks fourth for tumor-related mortality annually worldwide [1]. In recent years, great progress has been made in the detection and treatment of GC by technological and treatment advances. However, the morbidity rate of GC remains high because of postoperative recurrence and metastasis. Therefore, finding novel molecular biomarkers to predict the prognosis as well as therapeutic targets of GC is urgent.

Autophagy is a highly conserved process during the evolution of cell decomposition, which plays an essential role in regulating cell growth and internal homeostasis [2], and performs various functions in benign diseases and malignant tumors. For example, activation of mitophagy, which is a specific form of autophagy in macrophages, has major roles in ameliorating atherosclerosis progression [3]. Autophagy also increases the chemotherapeutic drug resistance and metastasis of tumor cells by enhancing their mobility and anoikis resistance [4–9]. Wang et al. showed that increased autophagy combined with multifunctional nanoparticles enhances drug accumulation and effectively treats deep tumor cells [10]. However, several studies have reported that autophagy inhibits cell proliferation

* Corresponding author.

E-mail address: xcf601@163.com (C. Xu).

<https://doi.org/10.1016/j.heliyon.2023.e16735>

Received 11 January 2023; Received in revised form 24 May 2023; Accepted 25 May 2023

Available online 29 May 2023

2405-8440/© 2023 The Authors. Published by Elsevier Ltd. This is an open access article under the CC BY-NC-ND license (<http://creativecommons.org/licenses/by-nc-nd/4.0/>).

and enhances tumor cell chemosensitivity to induce cell death [11]; Moreover, autophagy suppresses colorectal cancer (CRC) cells metastasis by inhibiting epithelial-mesenchymal transition (EMT) via the phosphoinositide 3-kinase/AKT signaling pathway [12]. Masuda et al. [13] found that autophagy was enhanced in GC patients and correlated to poor survival, especially in the early clinical stage. Luo et al. showed that activation of autophagy induces chemoresistance in GC [14]. Therefore, the mechanisms of autophagy in tumorigenesis and progression of GC require further study.

Microtubule-associated protein 1 light chain 3 (LC3), belonging to the LC3/GABARAP family of ubiquitin-like proteins, is involved in the formation of autophagosomes [15]. LC3B, an isoform of LC3, has been well investigated and found to be an autophagosome marker. When autophagy is activated, soluble LC3B-I is covalently conjugated to phosphatidylethanolamine and transforms into LC3B-II, which is critical for phagophore closure to form an autophagosome [16]. p62, also known as sequestosome 1, mediates the linkage between cargos and autophagosomes via its ubiquitin-associated and LC3-interacting region domains, respectively, and it directly binds to LC3 and facilitates degradation of ubiquitinated protein aggregates via autophagy [17]. During this process, p62 itself is also degraded [18]. Therefore, LC3B-II/LC3B-I is elevated and p62 is decreased by enhanced autophagy. Chloroquine (CQ) inhibits autophagy by suppressing lysosomal functions and blocking autophagosome-lysosome fusion, leading to the accumulation of LC3B-II and p62 [19].

Mammalian sterile-20-like kinase 4 (MST4), which is also known as serine/threonine kinase 26 (STK26), belongs to germinal center kinase (GCK) group III family including MST1, MST2, MST3 and SOK1 [20]. MST4 is involved in normal cell polarity by phosphorylating the regulatory T567 residue of ezrin [21]. MST4 binds to Golgi matrix protein GM130 for targeting to the Golgi apparatus and regulating cell migration by modulating the morphology of the Golgi apparatus [22]. MST4 also promotes tumor cell migration and metastasis by activating the p-ERK signaling pathway and interacting with FAM40A, a STRIPAK element [23,24]. Overexpression of MST4 is strongly related to poor prognoses of several carcinomas including hepatocellular carcinoma, breast cancer, choriocarcinoma, and prostate cancer [25–27]. However, there is no consensus on the function of MST4 in GC. Li et al. found that MST4 promotes tumor cell metastasis by facilitating EMT and indicates a poor prognosis of GC patients [28]. However, An et al. demonstrated that MST4 suppresses GC tumorigenesis by attenuating YAP activation through a non-canonical signaling pathway [29].

In the present study, we ascertained the clinical significance of MST4 in GC and further explored the relationship between MST4 and tumor cell proliferation, invasion, and metastasis *in vitro* and *in vivo*.

2. Materials and methods

2.1. Patients and specimens

We obtained RNA-sequencing (RNA-seq) and clinical data of pan-cancer and the adjacent normal tissue from TCGA-Xena (<http://xena.ucsc.edu/>) to analyze the MST4 mRNA level of pan-cancer. We collected data from 213 consecutive GC patients who underwent radical gastrectomy at the First Affiliated Hospital of Wannan Medical College between January 2012 and December 2013. This study was approved by the ethics committee of the First Affiliated Hospital of Wannan Medical College (approval number: LLSC-2022-17) and complied with all regulations. Informed consent was obtained from all the participants. Patients were followed up for 5 years, and the average follow-up time was 49 months, ranging from 5 to 60 months. During the first year after surgery, patients were followed up every 6 months, and then once a year for the next 4 years. The definition of overall survival (OS) was the time from surgery to death attributed to GC or to the last observed date. Disease free survival (DFS) was defined as the time from surgery to GC recurrence or metastasis.

2.2. Immunohistochemistry

Histological sections were soaked in xylene for de-paraffinization, and then gradient ethanol was used for dehydration. Antigen retrieval was conducted in a microwave. Endogenous peroxidases were blocked by incubation in 3% H₂O₂. The sections were incubated with an anti-human MST4 rabbit monoclonal antibody (1:200, ab52491, Abcam, USA) overnight at 4 °C, followed by a secondary antibody labelled with HRP (Beyotime Biotechnology, Shanghai, China). DAB chromogenic reagent (Maixin Biotechnology, Fuzhou, China) was used for development. The sections were counterstained in with hematoxylin and then mounted. In accordance with the staining intensity of immunohistochemistry, sections were scored from 0 to 3: 0, no staining; 1, weak staining; 2, moderate staining; 3, strong staining. The extent of staining was scored from 0 to 3 by the proportion of stained tumor cells (0%–10%; 11%–50%; 51%–75%; >75%). The final score was obtained by the multiplying of intensity and extent score. A final score of <3 was deemed as low expression, and a final score of ≥3 was deemed as high expression.

2.3. Lentiviral vectors construction and infection

Lentiviral vectors encoding specific shRNAs against full-length MST4 and a non-targeted control vector were transfected into 293T cells using Lipofectamine 2000 (Invitrogen, USA). To obtain the stable cell lines, the viral supernatant was collected at 48–72 h after transfection and used to infect target cells. AGS cells were infected with lentiviruses expressing MST4 shRNA-1(5'-CACCGTAC-GAAAGAAGCCTGATCCA-3') and shRNA-2 (5'-GAGCAAGATCTTGTGCAAACCCTGA-3'), and BGC-823 and SGC-7901 cells were infected with lentiviruses expressing the human MST4 gene. After 48 h of transduction, polyclonal stable cells were selected with 2.5 µg/ml puromycin for 2 weeks for *in vitro* experiments and monoclonal stable cells were selected with 2.5 µg/ml puromycin for 4 weeks for xenografting *in vivo* experiments. Cells were harvested to detect MST4 mRNA and protein expression.

2.4. Real-time PCR (qRT-PCR)

Total RNA was extracted by TRIzol (Thermo Fisher Scientific, Shanghai, China). Reverse-transcription was performed using a Prime-Script 1st Strand cDNA Synthesis Kit (Takara Biotechnology, Dalian, China) in accordance with the manufacturer's instructions. The primer sequences used were as follows: MST4: forward primer, 5'-TTCGAGCTGGTCCATTGATG-3' and reverse primer, 5'-TGAATGCAGATAGTCCAGACCT-3'; GAPDH (control): forward primer: 5'-GTGAAGGT CCGAGTCAACG -3'; reverse primer: 5'-CTGGGAAGTAACTGGAGT -3'. The amplification steps were 95 °C for 30 s and then 40 cycles at 95 °C for 5 s and at 60 °C for 30 s. The $2^{-\Delta\Delta CT}$ method was applied for relative quantification of gene expression.

2.5. Western blotting (WB)

Proteins were extracted with RIPA lysis buffer (Beyotime Biotechnology), separated on a 10% sodium dodecyl sulfate-polyacrylamide gel (Beyotime Biotechnology), and transferred onto a polyvinylidene difluoride (PVDF) membrane. After blocking with 5% dry skimmed milk, the membranes were incubated with a primary antibody at 4 °C overnight and then washed twice with Tris-buffered saline containing Tween (Haoran Biotechnology Co., Ltd., Shanghai, China). After incubation with a peroxidase-conjugated secondary antibody, the membrane was developed by enhanced chemiluminescence (Pierce, USA), following the manufacturer's instructions. Antibodies used were as follows: anti-human MST4 (rabbit monoclonal, 1:1000; Abcam, USA); anti-human p62 (mouse monoclonal, 1:1000; Santa Cruz Biotechnology, USA), anti-human Slug (mouse monoclonal, 1:1000; Santa Cruz Biotechnology, USA); anti-human LC3B (rabbit monoclonal, 1:1000; Cell Signaling Technology, USA); anti-human E-cadherin (mouse monoclonal, 1:500; Beyotime Biotechnology); anti-human β -actin (mouse monoclonal, 1:1000; Abcam).

2.6. Cell proliferation assay

The Cell Counting Kit-8 (CCK-8) assay (Beyotime Biotechnology) was applied to estimate the cell proliferation. Cultured cells were seeded into 96-well plates at 5×10^3 cells per well in 100 μ l of medium. After cell adhesion, the cells were treated with 10 μ l CCK-8 reagent for 3 h. Absorbance at 450 nm was then measured with enzyme-linked immunosorbent analyzer following the manufacturer's protocol.

2.7. Colony formation assay

To assess the colony formation capacity, 1×10^3 logarithmically growing cells were seeded into a 6-well plate and cultured for 2 weeks. Then, 4% paraformaldehyde was used to fix the colonies, and crystal violet (Beyotime Biotechnology) was applied to stain the cells. Stained cells were photographed, and colonies were counted with Image J software.

2.8. Transwell migration and invasion assay

Matrigel (BD Biosciences, Bedford, MA, USA) diluted at 1:4 with serum-free RPMI-1640 medium was used to assess the invasive ability and omitted to assess the migratory ability. Cell suspensions (3×10^5 /ml) were prepared after 12 h of serum starvation. The lower chamber contained RPMI-1640 medium with 10% FBS, while the upper chamber contained serum-free medium. A cell suspension (100 μ l) was added to the upper chamber and incubated at 37 °C for 24 h. Cells were fixed with 4% paraformaldehyde and stained with 0.1% crystal violet. Cells on the bottom of the membrane were imaged under a microscope (Leica, USA).

2.9. Wound healing assay

Cells (1×10^6) were seeded into a 6-well plate and cultured until 90% confluence. A wound was made with a 10 μ l micropipette tip. Cells were monitored, and wound healing was photographed under an inverted microscope ($\times 100$ magnification) at 0 and 48 h after scratching.

2.10. Xenografts

BALB/c-nude mice (4–5 weeks old, 16–18 g) were purchased from the Animal Experimental Center of Anhui Medical University (Hefei, Anhui, China) and raised in the Animal Institute of Wannan Medical College (Wuhu, Anhui, China). All experimental procedures followed protocols approved by the Medical Experimental Animal Care and Use Committee of Wannan Medical College (approval number: LLSC-2022-066). Fifteen BALB/c-nu/nu mice were randomly divided into three groups (control, MST4-shRNA1, and MST4-shRNA2), and implanted with vector-infected AGS cells (5×10^6) into their left armpit. The tumor size (length and width) was measured with calipers twice a week. Tumor volume was calculated using formula $V (\text{mm}^3) = (\text{length} \times \text{width}^2)/2$. The mice were humanely euthanized after 6 weeks, and tumors were harvested and weighed. Real-time PCR and WB were performed to measure the MST4 expression level in the xenograft.

2.11. Statistical analysis

SPSS 26.0 (SPSS Inc., Chicago, IL, USA) was used for the statistical analysis. We used the R package “ggplot2” to draw the scatter plots. Categorical data analysis was performed using the chi-squared test or Fisher’s exact test. The Student’s *t*-test was used to analyze two groups of quantitative data. The Kaplan–Meier method with the log-rank test was applied for patient survival analysis. Cox regression analysis was applied to identify independent risk factors for prognosis. All in vitro experiments were performed in triplicate. Two-tailed $P < 0.05$ was considered statistically significant.

3. Results

3.1. MST4 is overexpressed in GC cell lines and GC tissue

We downloaded the pan-cancer data on tumor tissue and the adjacent normal tissue from the TCGA-Xena database. We found that MST4 mRNA expression was significantly higher in most of the tumor tissue compared with that in adjacent normal tissue including STAD (referred to GC) ($P < 0.001$) (Supplementary Fig. S1A). Moreover, Pearson correlation analysis of MST4 and pan-cancer from TCGA showed that MST4 is positively correlated to most of the 33 tumors containing GC (Supplementary Fig. S1B).

We conducted qRT-PCR and WB to determine the mRNA and protein levels of MST4 in normal gastric epithelial cells (NGEC) and four GC cell lines (AGS, BGC-823, SGC-7901, and MKN-45). The results showed that the MST4 mRNA and protein levels were higher in the four GC cell lines compared with those in NGEC. Interestingly, MST4 mRNA and protein levels were obviously higher in poorly differentiated cell lines AGS and MKN-45 than in the moderately differentiated cell line SGC-7901. (Fig. 1B and Fig. 1A). Poorly differentiated cells usually indicate highly invasive and metastatic features. These results suggested that high MST4 expression is involved in tumor progression by affecting the invasive capacity of GC cells.

Next, we performed qRT-PCR and WB to examine MST4 mRNA and protein expression in a typical sample of GC tissue and matched adjacent normal gastric mucosal tissue. Our results revealed that MST4 mRNA and protein were both highly expressed in GC tissue compared with those in normal gastric mucosal tissue, respectively (Supplementary Figs. S1C and 1D).

3.2. Upregulation of MST4 is associated with the clinicopathological characteristics of GC

MST4 was mainly located in the cytoplasm of GC cells. Stronger staining of MST4 was found in GC tissue compared with the staining in adjacent normal gastric mucosal tissue. (Fig. 1C). As shown in Table 1, MST4 expression was linked to the tumor size, invasion depth, histology, ulceration, lymph node metastasis, lymphovascular invasion, perineural invasion, and TNM stage (Table 1). Tumors with high expression of MST4 had deeper invasion and more lymph node metastasis, lymphovascular invasion, and perineural

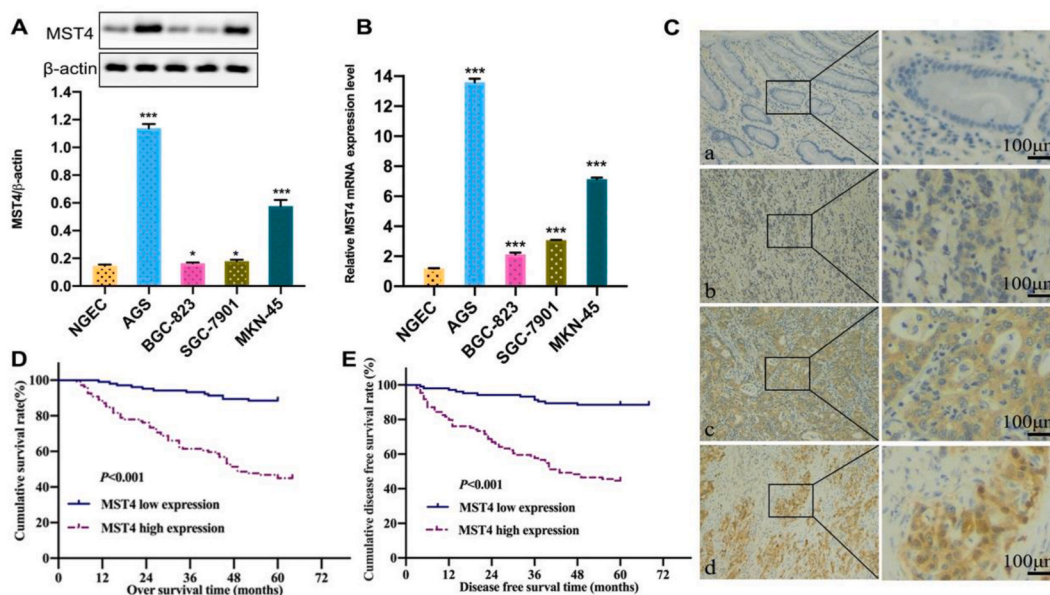


Fig. 1. MST4 protein and mRNA expression is increased in GC cell lines and tissue and correlated to poor clinical prognosis. A-B. MST4 protein expression level (A) and mRNA expression level (B) in NGEC and GC cell lines. C. Representative images of MST4 expression in adjacent normal gastric tissue (a. negatively staining) and GC tissue (b. low positive c. moderately positive d. strongly positive). D-E. Significant differences of OS (D) and DFS (E) between MST4 high and low expression groups of GC patients. The uncropped versions of Fig. A were provided as supplementary material. * $P < 0.05$ *** $P < 0.001$.

Table 1
Relationship between MST4 expression and patients' characteristics in GC.

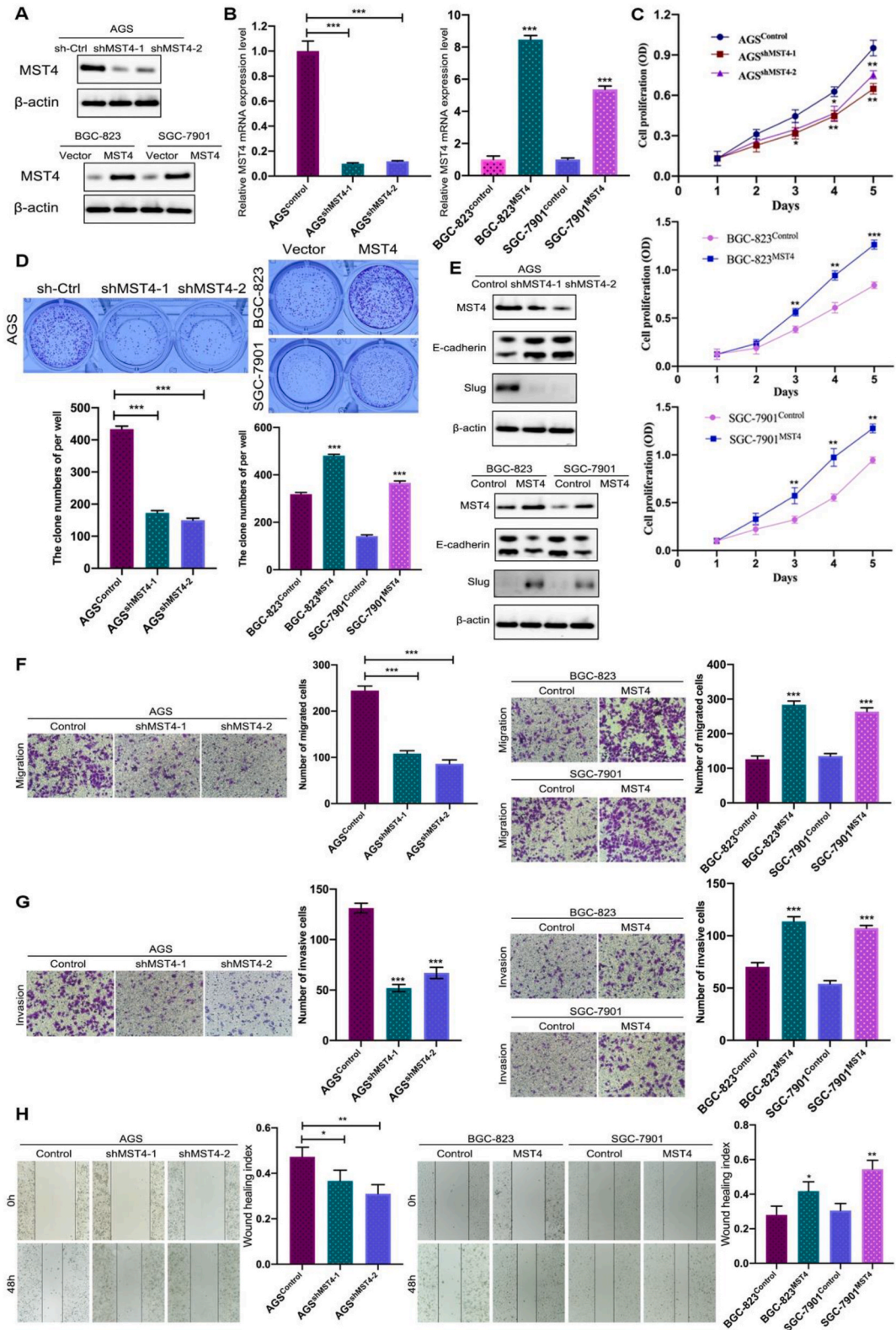
All	Total (N = 213)	MST4 low expression (n = 104)	MST4 high expression (n = 109)	P value
Age(years)				
mean ± SD	59.4 ± 10.6	59.2 ± 10.1	59.7 ± 11.1	0.731
Sex				0.499
Male	144(67.6)	68(65.4)	76(69.7)	
Female	69(32.4)	36(34.6)	33(30.3)	
Location				0.822
Upper third	49(23.0)	22(21.2)	27(24.8)	
Middle third	66(31.0)	33(31.7)	33(30.3)	
Lower third	98(46.0)	49(47.1)	49(45.0)	
Depth of invasion				<0.001
pT1	105(49.3)	76(73.1)	29(26.6)	
pT2	15(7.0)	8(7.7)	7(6.4)	
pT3	16(7.5)	4(3.8)	12(11.0)	
pT4	77(36.2)	16(15.4)	61(56.0)	
Tumor size(cm)				<0.001
mean ± SD	3.5 ± 1.9	2.6 ± 1.5	4.3 ± 2.0	0.008
Histological type				
Adenocarcinoma				
Well differentiated	5(2.3)	4(3.8)	1(0.9)	
Moderately differentiated	70(32.9)	43(41.3)	27(24.8)	
Poorly differentiated	121(56.8)	46(44.2)	75(68.8)	
Mucinous adenocarcinoma	12(5.6)	8(7.7)	4(3.7)	
Signet ring cell carcinoma	5(2.3)	3(2.9)	2(1.8)	
Ulceration				0.005
Absence	98(46.0)	58(55.8)	40(36.7)	
Presence	115(54.0)	46(44.2)	69(63.3)	
Lymph node metastasis				<0.001
Absence	87(40.8)	65(62.5)	22(20.2)	
Presence	126(59.2)	39(37.5)	87(79.8)	
Lymphovascular invasion				<0.001
Absence	152(71.4)	92(88.5)	60(55.0)	
Presence	61(28.6)	12(11.5)	49(45.0)	
Perineural invasion				<0.001
Absence	125(58.7)	83(79.8)	42(38.5)	
Presence	88(41.3)	21(20.2)	67(61.5)	
TNM Stage				<0.001
I	97(45.5)	75(72.1)	22(20.2)	
II	31(14.6)	10(9.6)	21(19.3)	
III	85(39.9)	19(18.3)	66(60.6)	

Data are presented as numbers (%)..

Table 2
Univariate and multivariate analyses for survival in GC patients.

Variable	Overall survival				Disease free survival			
	Univariate	Multivariate			Univariate	Multivariate		
	P value	P value	Hazard ratio	95% CI	P value	P value	Hazard ratio	95% CI
Histological type	0.000	NS			0.000	0.048	1.859	1.005–3.438
differentiated								
undifferentiated								
MST4 expression	<0.001	0.013		1.189–4.306	<0.001	0.011		1.216–4.413
Low expression			1				1	
High expression			2.263				2.316	
Depth of invasion	<0.001	NS			<0.001	NS		
Ulceration	<0.001	NS			<0.001	NS		
LNM	<0.001	0.029		1.161–15.521	<0.001	0.024		1.217–16.231
Absent			1				1	
Present			4.244				4.444	
LVI	<0.001	NS			<0.001	NS		
PI	<0.001	NS			<0.001	NS		
TNM Stage	<0.001	<0.001		2.080–7.883	<0.001	<0.001		2.061–7.842
I + II			1				1	
III			4.049				4.020	

CI, confidence interval; LNM, lymph node metastasis; LVI, lymphovascular invasion; PI, perineural invasion.



(caption on next page)

Fig. 2. MST4 enhances proliferation and invasion of GC cells in vitro. A-B. WB analysis of MST4 protein expression (A) and qRT-PCR analysis of MST4 mRNA expression (B) in AGS cells infected with MST4-shRNAs (Fig. A above panel and Fig. B left panel) and BGC-823 and SGC-7901 cells infected with lentiviruses expressing MST4 gene (Fig. A below panel and Fig. B right panel). C-D. CCK8 assay analysis (C) and colony formation analysis (D) of the proliferation of AGS cells downregulated MST4 (Fig. C above panel and Fig. D left panel) and BGC-823 and SGC-7901 cells upregulated MST4 (Fig. C below panel and Fig. D right panel). E. WB analysis of invasion associated proteins expression in GC cells downregulated and upregulated MST4. F-G. Transwell migration (F) and invasion (G) assay analysis of migration and invasion capacity of GC cells downregulated and upregulated MST4. H. Wound healing assay analysis of migration ability of AGS (right panel) and BGC-823 and SGC-7901 (left panel). The uncropped versions of Fig. A and E were provided as supplementary material. * $P < 0.05$; ** $P < 0.01$; *** $P < 0.001$.

invasion ($P < 0.001$). Overexpression of MST4 tended to indicate advanced tumor stages ($P < 0.001$). These results suggested that MST4 overexpression is correlated to the tumorigenesis and progression of GC.

3.3. Overexpression of MST4 in GC is associated with poor clinical outcomes

Kaplan–Meier survival analysis demonstrated that high expression of MST4 was correlated to shorter OS and DFS of GC patients. We found that the 5-year OS and DFS rate was obviously better in the low MST4 expression group compared with the rate in the high expression group ($P < 0.001$) (Fig. 1D and E). Multivariate Cox regression analysis indicated that MST4 overexpression was an independent risk factor for OS ($P = 0.013$) and DFS ($P = 0.011$) of GC (Table 2). These data demonstrated that high expression of MST4 in GC patients correlates to poor survival.

3.4. MST4 enhances proliferation and invasion of GC cells in vitro

As shown in Fig. 2A and B, MST4 protein and mRNA expression was downregulated in MST4-shRNA1 and MST4-shRNA2 groups compared with that in control group of AGS cells. CCK-8 and colony formation assays indicated that AGS cells proliferation was dramatically decreased by knockdown of MST4 (Fig. 2C and D). Moreover, the invasive capacity of AGS cells was reduced remarkably as suggested by transwell and wound healing assays (Fig. 2F–H). Next, MST4 was overexpressed in BGC-823 and SGC-7901 cells (Fig. 2A and B). As expected, CCK-8 and colony formation assays confirmed that proliferation was significantly enhanced by exogenous expression of MST4 in GC cells compared with the finding with the control (Fig. 2C and D). WB showed that MST4 upregulation led to the overexpression of Slug and low expression of E-cadherin, and vice versa in GC cells (Fig. 2E). Furthermore, transwell and wound healing assays showed that the invasive capacity was obviously increased by overexpression of MST4 in GC cells (Fig. 2F–H).

3.6. MST4 promotes tumorigenesis of GC in vivo

As shown in Fig. 3A, the ability of AGS cells with MST4 knockdown (MST4-shRNA1 and MST4-shRNA2 groups) to form tumors in nude mice was significantly decreased compared with that of empty vector-infected cells (control group), which was indicated by the

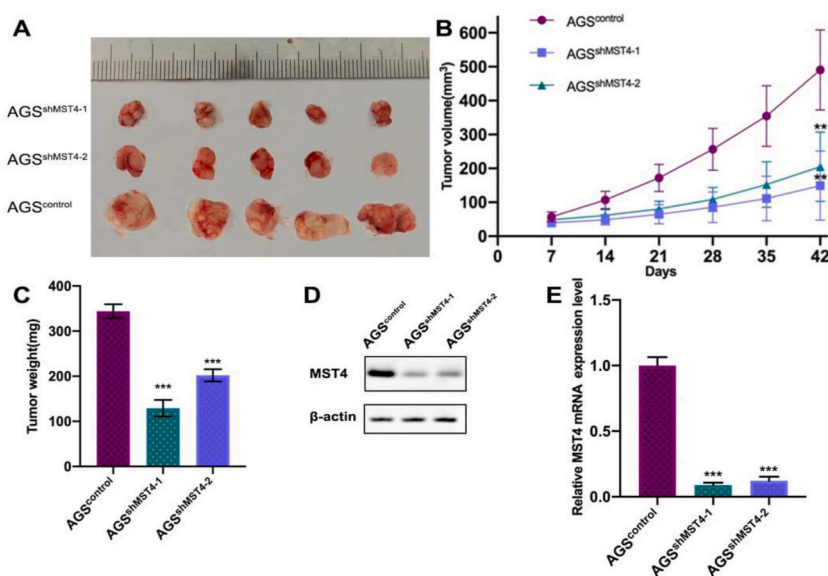
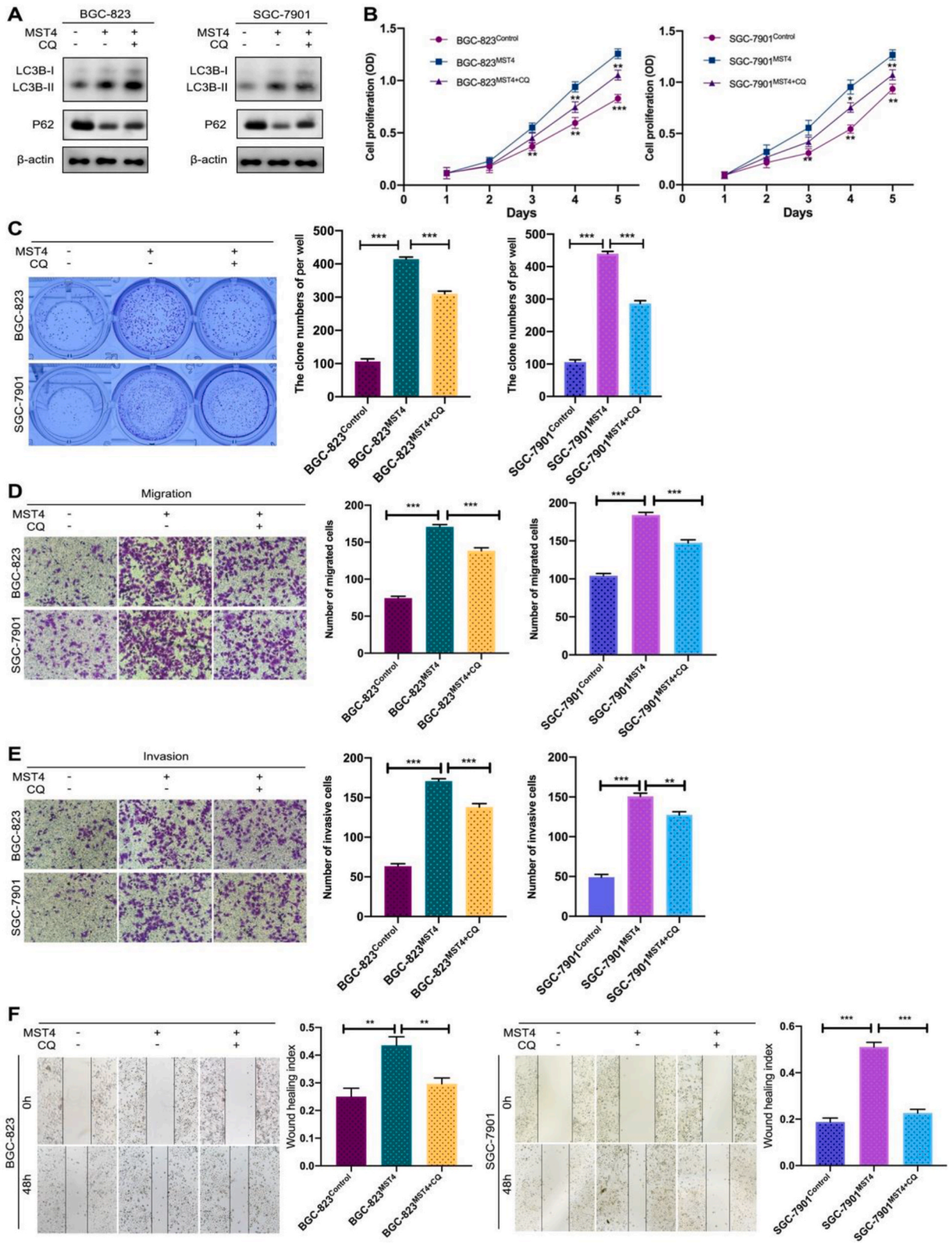


Fig. 3. MST4 regulates the tumorigenesis of GC. A. Images of excised tumors in various groups of BALB/c-nude mice. B. Tumor volumes were measured twice a week. C. Average weight of excised tumors in different groups. D-E. WB (D) and qRT-PCR (E) analysis of MST4 expression in excised tumors. The uncropped versions of Fig. D were provided as supplementary material. ** $P < 0.01$; *** $P < 0.001$.



(caption on next page)

Fig. 4. MST4 performs its function by promoting autophagy in GC. A. WB analysis of the autophagy associated proteins LC3B and p62 expression in BGC-823 and SGC-7901 cells. B–C. CCK8 (B) and colony formation assays (C) showed that CQ partly diminished the MST4-induced proliferation in BGC-823 and SGC-7901 cells. D–E. Transwell migration and invasion assay displayed CQ partly decreased the MST4-induced migration (D) and invasion (E) in BGC-823 and SGC-7901 cells. F. Wound healing assay showed the migration ability of BGC-823 and SGC-7901 cells was attenuated by CQ. The uncropped versions of Fig. A were provided as supplementary material. * $P < 0.05$; ** $P < 0.01$; *** $P < 0.001$.

xenograft tumor size, weight, and tumor growth curves (Fig. 3A, C and 3B). Real-time PCR and WB showed that MST4 expression in the tumors formed by shRNA-infected cells was obviously lower than that in the tumors formed by the empty vector-infected cells (Fig. 3E and D).

3.7. MST4 performs its function by promoting autophagy in GC

To identify the specific mechanism of MST4 in GC, we explored the link between MST4 and autophagy. Autophagy inhibitor chloroquine (CQ) (10 μmol ; Sigma-Aldrich, USA) was used to attenuate autophagic activity in BGC-823 and SGC-7901 cells overexpressing MST4. As shown in Fig. 4A, overexpression of MST4 in BGC-823 and SGC-7901 cells decreased p62 and increased LC3BII/LC3BI, indicating enhanced autophagy. CQ partly reversed the MST4-induced decrease in p62, but not to control levels. Furthermore, CQ further increased the LC3BII/LC3BI expression in GC cells (Fig. 4A). CQ treatment also decreased the proliferation and invasive capacity of BGC-823 and SGC-7901 cells with MST4 overexpression (Fig. 4B–F).

4. Discussion

Recurrence after radical gastrectomy is the main obstacle to improve the overall survival of GC patients, but its molecular mechanism has not been well understood until now. MST4 promotes proliferation and migration of various cancer cells via different mechanisms [26,30,31]. Arora et al. demonstrated that MST4 as an oncogene enhances cell growth and migration by promoting EMT via activating Akt in breast cancer [26]. Moreover, MST4 directly phosphorylates β -catenin to promote the tumor cell proliferation and is associated with a poor prognosis of CRC [30]. Moreover, the MST4-MOB4 complex regulates the Hippo-YAP pathway to promote growth and migration of pancreatic cancer cells [32]. However, the role of MST4 in GC remains controversial. A recent study suggested that MST4 is an oncogene and predicts a poor prognosis of GC patients [28], whereas another study revealed MST4 suppresses GC tumorigenesis by directly phosphorylating YAP [29]. We aimed to ascertain the clinical significance of MST4 in GC and explore its roles in vitro and in vivo.

Consistent with a previous study [28], we found that MST4 mRNA and protein expression was distinctly higher in GC cell lines and tissue. Furthermore, we revealed that upregulation of MST4 was related to the tumor size, invasion depth, histology, ulceration, lymph node metastasis, lymphovascular invasion, perineural invasion, and TNM stage, and MST4 was an independent prognostic indicator for GC patients. These results indicated that MST4 might act as an oncogene and is involved in tumor progression of GC via enhancing cell proliferation and invasion.

To confirm the MST4 function in GC, we performed a series of in vitro and in vivo experiments. Our results revealed that upregulation of MST4 promoted proliferation and facilitated the invasion and migration of GC cells, and vice versa. Moreover, MST4 overexpression increased Slug expression and decreased E-cadherin expression. Because Slug and E-cadherin are markers of EMT [33], our data suggested that MST4 promoted cell migration and invasion via EMT. Furthermore, we showed that downregulation of MST4 attenuated tumor growth in vivo.

Recent studies have suggested that autophagy plays major roles in tumor cell proliferation and invasion via different signaling pathways. Autophagy inhibition regulated by MCOLN1/TRPML1 suppresses melanoma cell migration and invasion by regulating a ROS-induced TP53/p53 pathway [9]. Another recent study showed that UPR-induced autophagy driven by Sec62 increases the GC invasive ability [34]. Wu et al. demonstrated that SphK1-induced autophagy enhances focal adhesion paxillin-mediated metastasis of CRC [35]. MST4 stimulates autophagy by phosphorylating ATG4B to promote the tumorigenicity of glioblastoma [31]. However, an association between MST4 and autophagy has not been demonstrated in GC. We found that upregulation of MST4 lead to p62 downregulation and LC3BII/LC3BI increasing, indicating enhanced autophagy, and thus increased the proliferation and invasive capacity of GC cells. Moreover, because autophagy was inhibited by CQ in MST4-overexpressing GC cells, the proliferation and invasive potential was decreased. Thus, we inferred that the MST4 is a major protein in promoting tumor development at least partly via inducing autophagy in GC. While the specific mechanism of MST4 regulating autophagy was not investigated, and it will be further explored in our future studies.

5. Conclusion

Overexpression of MST4 in GC patients predicted poor clinical outcomes. MST4 enhanced the proliferation and migration of GC cells in vitro and in vivo. MST4 facilitated proliferation and invasion of GC cell by enhancing autophagy. Thus, MST4 may be a potential prognostic and therapeutic candidate for GC.

Ethical approval and consent to participate

This study gained the approval of the ethics committee of the First Affiliated Hospital of Wannan Medical College (approval number: LLSC-2022-17) and the Medical Experimental Animal Care and Use Committee of Wannan Medical College (approval number: LLSC-2022-066), meanwhile the study complies with all regulations.

Author contribution statement

Pengwei Liu: Performed the experiments; Wrote the paper. Lin Li; Wei Wang: Analyzed and interpreted the data. Chiyi He: Contributed reagents, materials, analysis tools or data. Chunfang Xu: Conceived and designed the experiments.

Declaration of competing interest

The authors declare that they have no known competing financial interests or personal relationships that could have appeared to influence the work reported in this paper.

Acknowledgments

The authors acknowledge support from the Key Natural Science Foundation Project of Wannan Medical College (Grant No. WK2021ZF18, WK2022ZF03), Wuhu City Science and Technology Project (Grant No. 22021yf63), and Key Research and Development Program Project of Anhui Province (Grant No. 201904a07020028).

Appendix A. Supplementary data

Supplementary data to this article can be found online at <https://doi.org/10.1016/j.heliyon.2023.e16735>.

References

- [1] H. Sung, et al., Global cancer statistics 2020: GLOBOCAN estimates of incidence and mortality worldwide for 36 cancers in 185 countries, *CA A Cancer J. Clin.* 71 (2021) 209–249, <https://doi.org/10.3322/caac.21660>.
- [2] A.R. Ariosa, et al., A perspective on the role of autophagy in cancer, *Biochim. Biophys. Acta, Mol. Basis Dis.* 1867 (2021), 166262, <https://doi.org/10.1016/j.bbdis.2021.166262>.
- [3] A. Ajoolahbady, et al., Melatonin-based therapeutics for atherosclerotic lesions and beyond: focusing on macrophage mitophagy, *Pharmacol. Res.* 176 (2022), 106072, <https://doi.org/10.1016/j.phrs.2022.106072>.
- [4] Y.S. Abd El-Aziz, et al., Autophagy: a promising target for triple negative breast cancers, *Pharmacol. Res.* 175 (2022), 106006, <https://doi.org/10.1016/j.phrs.2021.106006>.
- [5] Y. Yu, et al., ATF4/CEMIP/PKCalpha promotes anoikis resistance by enhancing protective autophagy in prostate cancer cells, *Cell Death Dis.* 13 (2022) 46, <https://doi.org/10.1038/s41419-021-04494-x>.
- [6] S. Wang, et al., Acidic extracellular pH induces autophagy to promote anoikis resistance of hepatocellular carcinoma cells via downregulation of miR-3663-3p, *J. Cancer* 12 (2021) 3418–3426, <https://doi.org/10.7150/jca.51849>.
- [7] J. Xia, et al., NEK2 induces autophagy-mediated bortezomib resistance by stabilizing Beclin-1 in multiple myeloma, *Mol. Oncol.* 14 (2020) 763–778, <https://doi.org/10.1002/1878-0261.12641>.
- [8] W.Q. Yang, et al., Inhibition of bromodomain-containing protein 4 enhances the migration of esophageal squamous cell carcinoma cells by inducing cell autophagy, *World J. Gastrointest. Oncol.* 14 (2022) 2340–2352, <https://doi.org/10.4251/wjgo.v14.i12.2340>.
- [9] Y. Xing, et al., Autophagy inhibition mediated by MCOLN1/TRPML1 suppresses cancer metastasis via regulating a ROS-driven TP53/p53 pathway, *Autophagy* 18 (2022) 1932–1954, <https://doi.org/10.1080/15548627.2021.2008752>.
- [10] F. Wang, et al., Autophagy responsive intra-intercellular delivery nanoparticles for effective deep solid tumor penetration, *J. Nanobiotechnol.* 20 (2022) 300, <https://doi.org/10.1186/s12951-022-01514-6>.
- [11] T. Liu, et al., Momelotinib sensitizes glioblastoma cells to temozolomide by enhancement of autophagy via JAK2/STAT3 inhibition, *Oncol. Rep.* 41 (2019) 1883–1892, <https://doi.org/10.3892/or.2019.6970>.
- [12] Z. Ma, S. Lou, Z. Jiang, PHLDA2 regulates EMT and autophagy in colorectal cancer via the PI3K/AKT signaling pathway, *Aging (Albany NY)* 12 (2020) 7985–8000, <https://doi.org/10.18632/aging.103117>.
- [13] G.O. Masuda, et al., Clinicopathological correlations of autophagy-related proteins LC3, beclin 1 and p62 in gastric cancer, *Anticancer Res.* 36 (2016) 129–136.
- [14] Y. Luo, et al., Long noncoding RNA (lncRNA) EIF3J-DT induces chemoresistance of gastric cancer via autophagy activation, *Autophagy* 17 (2021) 4083–4101, <https://doi.org/10.1080/15548627.2021.1901204>.
- [15] X. Li, S. He, B. Ma, Autophagy and autophagy-related proteins in cancer, *Mol. Cancer* 19 (2020) 12, <https://doi.org/10.1186/s12943-020-1138-4>.
- [16] H.J. Hwang, et al., LC3B is an RNA-binding protein to trigger rapid mRNA degradation during autophagy, *Nat. Commun.* 13 (2022) 1436, <https://doi.org/10.1038/s41467-022-29139-1>.
- [17] S. Pankiv, et al., p62/SQSTM1 binds directly to Atg8/LC3 to facilitate degradation of ubiquitinated protein aggregates by autophagy, *J. Biol. Chem.* 282 (2007) 24131–24145, <https://doi.org/10.1074/jbc.M702824200>.
- [18] A. Vainstein, P. Grumati, Selective autophagy by close encounters of the ubiquitin kind, *Cells* 9 (2020), <https://doi.org/10.3390/cells9112349>.
- [19] J. Xu, et al., Chloroquine treatment induces secretion of autophagy-related proteins and inclusion of Atg8-family proteins in distinct extracellular vesicle populations, *Autophagy* 18 (2022) 2547–2560, <https://doi.org/10.1080/15548627.2022.2039535>.
- [20] Z. Qian, et al., Cloning and characterization of MST4, a novel Ste20-like kinase, *J. Biol. Chem.* 276 (2001) 22439–22445, <https://doi.org/10.1074/jbc.M009323200>.
- [21] W.C. Hao, et al., MST4 inhibits human hepatocellular carcinoma cell proliferation and induces cell cycle arrest via suppression of PI3K/AKT pathway, *J. Cancer* 11 (2020) 5106–5117, <https://doi.org/10.7150/jca.45822>.

- [22] C. Preisinger, et al., YSK1 is activated by the Golgi matrix protein GM130 and plays a role in cell migration through its substrate 14-3-3zeta, *J. Cell Biol.* 164 (2004) 1009–1020, <https://doi.org/10.1083/jcb.200310061>.
- [23] Z.H. Lin, et al., MST4 promotes hepatocellular carcinoma epithelial-mesenchymal transition and metastasis via activation of the p-ERK pathway, *Int. J. Oncol.* 45 (2014) 629–640, <https://doi.org/10.3892/ijo.2014.2455>.
- [24] C.D. Madsen, et al., STRIPAK components determine mode of cancer cell migration and metastasis, *Nat. Cell Biol.* 17 (2015) 68–80, <https://doi.org/10.1038/ncb3083>.
- [25] M.J. Dian, et al., MST4 negatively regulates the EMT, invasion and metastasis of HCC cells by inactivating PI3K/AKT/Snail1 axis, *J. Cancer* 12 (2021) 4463–4477, <https://doi.org/10.7150/jca.60008>.
- [26] R. Arora, et al., MST4: a potential oncogene and therapeutic target in breast cancer, *Cells* 11 (2022), <https://doi.org/10.3390/cells11244057>.
- [27] J. Baj, et al., Mechanisms of the epithelial-mesenchymal transition and tumor microenvironment in *Helicobacter pylori*-induced gastric cancer, *Cells* 9 (2020), <https://doi.org/10.3390/cells9041055>.
- [28] T. Li, et al., MST4 predicts poor prognosis and promotes metastasis by facilitating epithelial–mesenchymal transition in gastric cancer, *Cancer Manag. Res.* 11 (2019) 9353–9369, <https://doi.org/10.2147/cmar.S219689>.
- [29] L. An, et al., MST4 kinase suppresses gastric tumorigenesis by limiting YAP activation via a non-canonical pathway, *J. Exp. Med.* 217 (2020), <https://doi.org/10.1084/jem.20191817>.
- [30] H. Zhang, et al., An MST4-pbeta-catenin(Thr40) signaling Axis controls intestinal stem cell and tumorigenesis, *Adv. Sci.* 8 (2021), e2004850, <https://doi.org/10.1002/advs.202004850>.
- [31] T. Huang, et al., MST4 phosphorylation of ATG4B regulates autophagic activity, tumorigenicity, and radioresistance in glioblastoma, *Cancer Cell* 32 (2017) 840–855 e8, <https://doi.org/10.1016/j.ccell.2017.11.005>.
- [32] M. Chen, et al., The MST4-MOB4 complex disrupts the MST1-MOB1 complex in the Hippo-YAP pathway and plays a pro-oncogenic role in pancreatic cancer, *J. Biol. Chem.* 293 (2018) 14455–14469, <https://doi.org/10.1074/jbc.RA118.003279>.
- [33] K. Tripathi, et al., Immunohistochemical expressions of EMT markers in pan-RAS-pERK1/2-positive tumors improve diagnosis and prognosis assessment of non-muscle invasive bladder cancer and muscle invasive bladder cancer patients, *Mol. Cell. Biochem.* (2022), <https://doi.org/10.1007/s11010-022-04579-x>.
- [34] S. Su, et al., Sec62 promotes gastric cancer metastasis through mediating UPR-induced autophagy activation, *Cell. Mol. Life Sci.* 79 (2022) 133, <https://doi.org/10.1007/s00018-022-04143-2>.
- [35] J.N. Wu, et al., SphK1-driven autophagy potentiates focal adhesion paxillin-mediated metastasis in colorectal cancer, *Cancer Med.* 10 (2021) 6010–6021, <https://doi.org/10.1002/cam4.4129>.